

Inflationary quasiparticle creation and thermalization dynamics in coupled Bose-Einstein condensates

Anna Posazhennikova,^{1,*} Mauricio Trujillo-Martinez,² and Johann Kroha^{2,†}

¹*Department of Physics, Royal Holloway, University of London, Egham, Surrey TW20 0EX, United Kingdom*

²*Physikalisches Institut and Bethe Center for Theoretical Physics, Universität Bonn, Nussallee, 12, D-53115 Bonn, Germany*

(Dated: December 3, 2024)

A bosonic Josephson junction is a prototype system to investigate how (if at all) an isolated quantum system driven out of equilibrium reaches a steady and possibly thermalized state for long times. The relaxation happens because of the quasiparticle excitations induced by the initial quenching of the Josephson coupling. We describe such a coupled BEC and incoherent excitations system in terms of the quantum kinetic equations and analyse in detail system's nonequilibrium dynamics. We find, interestingly, that the nonequilibrium dynamics is governed by three different time scales. After an initial period τ_c of undamped Josephson oscillations, quasiparticles are created in an avalanche manner due to a dynamically generated parametric resonance between the Josephson frequency and the quasiparticle excitation energies. This leads to a fast depletion as well as damping of the BEC amplitude. When the final number of quasiparticles, allowed by total energy conservation, is reached, however, the quasiparticle system effectively decouples from the BEC oscillations (freeze-out time of the BEC τ_f), and the total quasiparticle number becomes nearly conserved. Under this approximate conservation law the system enters into a quasi-hydrodynamical regime which is characterized by a slow, exponential relaxation of the quasiparticle system into a thermalized state with thermalization time τ_{th} . We prove this behavior by a detailed Fourier analysis of the oscillatory behavior in the different time regimes.

PACS numbers: 67.85.-d, 67.85.De, 03.75.Lm

Experimental realisation of fully controllable systems of ultra cold gases relaunched interest in fundamental non-equilibrium problems, such as for example, relaxation and eventual thermalization of finite, isolated quantum systems [1, 2]. It seems that thermalization, if it happens, strongly depends on the system, and it is difficult to find a unique answer to the problem. For example, some low-dimensional systems thermalise very slowly and prior to thermalisation enter a so-called prethermalization regime, which became a topic of research by itself (see [3] and references therein). A bosonic Josephson junction created by loading a Bose-Einstein condensate (BEC) into a double-well trap [4–6], can serve as a paradigm for investigating of how a nonequilibrium quantum system relaxes and reaches thermal state, if at all. Time scales involved in the quasiparticle creation, the damping of the BEC oscillations and the eventual thermalisation of the quasiparticles in more than one-dimensional traps, where a true BEC exists, have been obscure. It is also clear that quasiparticle non-elastic collisions responsible for the system relaxation require a many-body field theoretical approach and are not captured by semiclassical descriptions [6], as also numerical studies indicate [7].

In this paper we study the nonequilibrium dynamics of the coupled BEC and incoherent excitations in detail. We derive the quantum kinetic equations using the

Bogoliubov-Keldysh Green's function technique [8, 9] in the time domain and representing the Hamiltonian in the discrete eigenbasis of the finite-size trap potential. Whereas the BECs in the double well are treated as classical amplitudes, the full quantum dynamics due to inelastic collisions of the incoherent excitations is taken into account.

We find rich dynamics governed by three main time scales. First of all, although we quench the Josephson coupling at the initial time $J(t) = J\theta(t)$, quasiparticles do not get excited simultaneously, but only after a certain time τ_c of multiple undamped Josephson oscillations, and in an avalanche-like, inflationary way [10, 11]. This results in a broad spectrum of the condensate oscillations which roughly corresponds to the spectrum of incoherent excitations in this regime. We attribute this curious behaviour to a dynamically generated parametric resonance between the Josephson frequency and the quasiparticle excitation energies. This "coupling" regime lasts till $\tau_f > \tau_c$ when effective decoupling of condensate modes and quasiparticles happens. The second energy scale τ_f comes into play because the number of excited quasiparticles is restricted from above due to the total energy conservation. Whenever the final number is reached, the crossover to the off-resonant regime takes place, BEC gets "frozen-out" and for $t > \tau_f$ the total quasiparticle number is effectively conserved. The new regime can be approximated as hydrodynamic and is characterized by a progressive exponential relaxation of the quasiparticle system towards a thermalized state. The third time-scale $\tau_{th} \gg \tau_f$ is the thermalization time in this regime.

*Email: anna.posazhennikova@rhul.ac.uk

†Email: kroha@th.physik.uni-bonn.de

We develop a semi-analytical field theoretical approach to the problem, applicable to any dimensionality and number of particles. In our approach the condensate is described within a semiclassical two-mode approximation [12], while quasi-particle contributions are described quantum-mechanically [10, 11]. We consider a BEC confined in a double-well potential with an initial population imbalance between the right and the left well: $z(0) = \frac{N_1(0) - N_2(0)}{N_1(0) + N_2(0)} \neq 0$ ($N_{1,2}(t)$ is the number of particles in the left (right) well). This system is known to exhibit Josephson oscillations [4, 5, 12]. It is most generally described by the standard Hamiltonian

$$H = \int d\mathbf{r} \hat{\Psi}^\dagger(\mathbf{r}, t) \left(-\frac{\nabla^2}{2m} + V_{ext}(\mathbf{r}, t) \right) \hat{\Psi}(\mathbf{r}, t) \quad (1)$$

$$+ \frac{g}{2} \int d\mathbf{r} \hat{\Psi}^\dagger(\mathbf{r}, t) \hat{\Psi}^\dagger(\mathbf{r}, t) \hat{\Psi}(\mathbf{r}, t) \hat{\Psi}(\mathbf{r}, t),$$

where $\hat{\Psi}(\mathbf{r}, t)$ is a bosonic field operator, and we assumed a contact interaction between the bosons with $g = 4\pi a_s/m$ (a_s is the s-wave scattering length). V_{ext} is the external double-well trapping potential. To obtain an effective Hamiltonian for our problem, we assume that our double well potential has discrete eigenstates and expand the field operator $\hat{\Psi}(\mathbf{r}, t)$ in terms of a complete basis $\mathbb{B} = \{\varphi_-, \varphi_+, \varphi_1, \varphi_2, \dots, \varphi_M\}$ of the exact single-particle eigenstates of $V_{ext}(\mathbf{r}, t > 0)$ after the coupling between the wells is turned on [11]:

$$\hat{\Psi}(\mathbf{r}, t) = \phi_1(\mathbf{r})a_1(t) + \phi_2(\mathbf{r})a_2(t) + \sum_{n=1}^M \varphi_n(\mathbf{r})\hat{b}_n(t), \quad (2)$$

The first two terms in Eq. (2) constitute the usual two-mode approximation for a condensate in a double well [12], i.e. ϕ_1 and ϕ_2 are symmetric and antisymmetric combinations of φ_- and φ_+ . The Bogoliubov substitution neglects phase fluctuations in the ground states of each of the potential wells, while the full quantum dynamics is taken into account for the excited states, φ_n , $n = 1, 2, \dots, M$. This is justified when the BEC particle numbers are sufficiently large, $N_\alpha \gg 1$, e.g., for the experiments [4]. In the numerical evaluations we will limit the number of levels which can be occupied by the quasi-particles to $M = 5$. And $a_{1,2} = \sqrt{N_{1,2}(t)} \exp(i\theta_{1,2}(t))$.

At time $t = 0$ the barrier between the wells is suddenly lowered, and a Josephson link is established between the two wells. The Hamiltonian for our system for $t > 0$ is then

$$H = H_{coh} + H_J + H_{coll}. \quad (3)$$

Here H_{coh} includes all coherent contributions, i.e. all the contributions which are bi-linear in \hat{b}_n -operators and local in α -index

$$H_{coh} = E_0 \sum_{\alpha=1}^2 a_\alpha^* a_\alpha + \frac{U}{2} \sum_{\alpha=1}^2 a_\alpha^* a_\alpha^* a_\alpha a_\alpha + \sum_{n=1}^M \epsilon_n \hat{b}_n^\dagger \hat{b}_n$$

$$+ K \sum_{\alpha=1}^2 \sum_{n,m=1}^M \left[a_\alpha^* a_\alpha \hat{b}_n^\dagger \hat{b}_m + \frac{1}{4} (a_\alpha^* a_\alpha^* \hat{b}_n \hat{b}_m + h.c.) \right], \quad (4)$$

where U and K are positive interaction constants, and ϵ_n are energies of 5 equidistant levels of the double well: $\epsilon_n = n\Delta$ with Δ being the level spacing.

H_J encompasses the Josephson terms, which are still coherent but are non-local in the α -index

$$H_J = -J(a_1^* a_2 + a_2^* a_1) + J' \sum_{n,m=1}^M \left[(a_1^* a_2 + a_2^* a_1) \hat{b}_n^\dagger \hat{b}_m \right.$$

$$\left. + \frac{1}{2} (a_1^* a_2^* \hat{b}_n \hat{b}_m + h.c.) \right], \quad (5)$$

where terms proportional to J' constitute quasiparticle assisted tunneling between the wells.

Finally, collisional terms H_{coll} account for the non-linear terms describing real interactions of quasiparticles

$$H_{coll} = \frac{U'}{2} \sum_{n,m=1}^M \sum_{l,s=1}^M \hat{b}_m^\dagger \hat{b}_n^\dagger \hat{b}_l \hat{b}_s$$

$$+ R \left[\sum_{\alpha=1}^2 \sum_{n,m,s=1}^M a_\alpha^* \hat{b}_n^\dagger \hat{b}_m \hat{b}_s + \sum_{\alpha,\beta,\gamma+1}^2 \sum_{n=1}^M a_\alpha^* a_\beta^* a_\gamma \hat{b}_n + h.c. \right] \quad (6)$$

Hereafter all our energies are counted from E_0 .

With the Hamiltonian we derive quantum kinetic equations for the classical \mathbf{C} and quantum \mathbf{G} parts of the Green's functions following standard field-theoretical techniques [8, 9]

$$\mathbf{C}_{\alpha\beta}(t, t') = -i \begin{pmatrix} a_\alpha(t) a_\beta^*(t') & a_\alpha(t) a_\beta(t') \\ a_\alpha^*(t) a_\beta^*(t') & a_\alpha^*(t) a_\beta(t') \end{pmatrix}, \quad (7)$$

$$\mathbf{G}_{nm}(t, t') = -i \begin{pmatrix} \langle T_C \hat{b}_n(t) \hat{b}_m^\dagger(t') \rangle & \langle T_C \hat{b}_n(t) \hat{b}_m(t') \rangle \\ \langle T_C \hat{b}_n^\dagger(t) \hat{b}_m^\dagger(t') \rangle & \langle T_C \hat{b}_n^\dagger(t) \hat{b}_m(t') \rangle \end{pmatrix}$$

where time ordering T_C is performed along the Keldysh contour. The Dyson equations for these function are

$$\int_C d\bar{t} [\mathbf{G}_0^{-1}(t, \bar{t}) - \mathbf{S}^{HF}(t, \bar{t})] \mathbf{C}(\bar{t}, t')$$

$$= \int_C d\bar{t} \mathbf{S}(t, \bar{t}) \mathbf{C}(\bar{t}, t'), \quad (8)$$

$$\int_C d\bar{t} [\mathbf{G}_0^{-1}(t, \bar{t}) - \mathbf{\Sigma}^{HF}(t, \bar{t})] \mathbf{G}(\bar{t}, t') = \mathbf{1} \delta(t - t')$$

$$+ \int_C d\bar{t} \mathbf{\Sigma}(t, \bar{t}) \mathbf{G}(\bar{t}, t'), \quad (9)$$

where we separated the first order Hartree-Fock self-energy contributions $\mathbf{S}^{HF}, \mathbf{\Sigma}^{HF}$ from their second order collisional counter-parts $\mathbf{S}, \mathbf{\Sigma}$. We then rewrite these Dyson equations in terms of spectral function $\mathbf{A}_{nm}(t, t') = i(\mathbf{G}_{nm}^>(t, t') - \mathbf{G}_{nm}^<(t, t'))$ and statistical function $\mathbf{F}_{nm}(t, t') = (\mathbf{G}_{nm}^>(t, t') + \mathbf{G}_{nm}^<(t, t'))/2 = \mathbf{G}_{nm}^K(t, t')/2$ and the corresponding self-energies (see Supplementary Materials). We solve the final integro-differential equations numerically for different initial conditions $z(0), \theta(0)$, total number of particles N_{tot} , inter-level spacing Δ and interactions U, U', K, J' and R , all

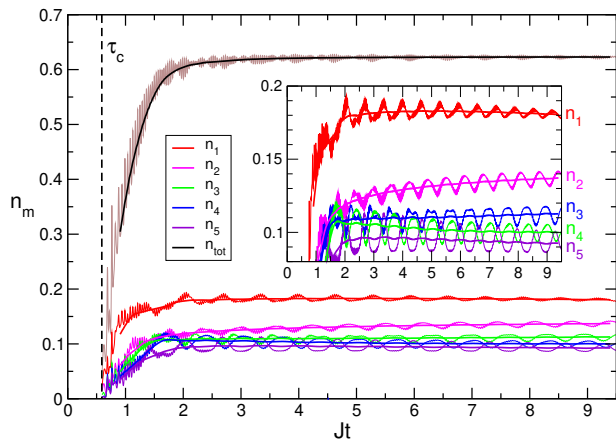


FIG. 1: Dynamics of incoherent excitations for $z(0) = 0.6$, $\theta(0) = 0$, and $\Delta = 9$, $u = u' = 5$, $j' = 40$, $N_{tot} = 5 \cdot 10^5$. n_m is the occupation number of the m -th level, n_{tot} is the sum of all 5 levels. $\tau_c \approx 0.59$ is the characteristic time scale at which the inflationary quasiparticle creation takes place. In the inset is the same plot but without n_{tot} for better visibility of the oscillations and the averages.

energy scales being expressed in the units of J : $u = UN_{tot}/J$, $u' = U'N_{tot}/J$, $k = KN_{tot}/J$, $j' = J'N_{tot}/J$, $r = RN_{tot}/J$.

In Fig. 1 we present our results for the dynamics of incoherent excitations for a certain parameter set. The oscillating with time occupation numbers of all five levels n_1, n_2, \dots, n_5 and their total

$$n_{tot}(t) = \sum_{m=1}^5 n_m(t) = - \sum_{m=1}^5 \Im F_{mm}^G(t, t) - \frac{5}{2}. \quad (10)$$

are shown for convenience along with their averages (see the thick lines on top of the oscillating ones). Here F_{mm}^G is the upper left component of the statistical Green's function \mathbf{F}_{mm} in the Bogoliubov space (see Supplementary Material). All n_m -s and n_{qp} are normalised by the total particle number $N_{tot} = N_1(0) + N_2(0)$. One can readily see the quasi saturation of quasiparticle occupation numbers for $t \gg \tau_c$.

In order to better understand this behaviour and to extract the second time scale, we plot the $\ln|n_{avg}(t) - n_{avg}(\infty)|$, $\ln|\Delta n(t)|$, and $\ln|z(t)|$ versus dimensionless time Jt (respectively upper, middle and lower panels in Fig. 2). n_{avg} is the averaged n_{tot} , and $n_{avg}(10) \approx n_{avg}(\infty)$ is the saturation value of n_{tot} , and $\Delta n(t) = n_{tot}(t) - n_{avg}(\infty)$. By making linear fits, one can see that exponential decay is described by two different decay rates. The change in decay happens at τ_f , the "freezing-out" time scale, which marks the onset of the quasiparticle saturation phase where incoherent excitations become decoupled from the coherent condensation modes. Thermalization time $\tau_{th} \gg \tau_f$ is the inverse decay rate in the decoupled, hydrodynamic-like regime.

From spectral and statistical functions of the quasiparticles we can now analyse the spectra of our system. We

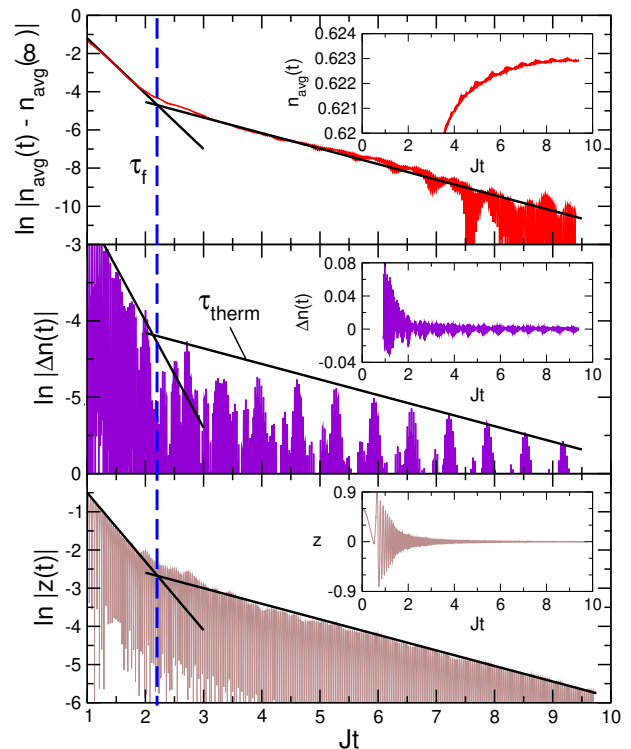


FIG. 2: Time-dependent averaged total quasiparticle number n_{avg} and the particle imbalance between BECs $z(t)$ (in the insets) and their natural logarithms. $n_{avg}(\infty) \approx n_{avg}(10)$, and $\Delta n(t) = n_{tot}(t) - n_{avg}(\infty)$. The dashed vertical line corresponds to τ_f and marks the crossover to the quasi-hydrodynamic regime.

implement Wigner mixed coordinates for the time arguments in the standard way: $t_- = t - t'$ and $t_+ = (t + t')/2$. We then Fourier transform $A^G(t_-, t_+) = \sum_n A_{nn}^G(t_-, t_+)$ and $F^G(t_-, t_+) = \sum_n F_{nn}^G(t_-, t_+)$ with respect to t_- and obtain frequency-dependent $A^G(\omega, t_+)$ and $F^G(\omega, t_+)$. In Fig. 3 we plot the frequency dependent absolute values of $|A^G(\omega, t_+)| \equiv |A(\omega)|$ and $|F^G(\omega, t_+)| \equiv |F(\omega)|$ for $t_+ = 9.01$, i.e. for relatively large times when the system is close to the equilibrium state. As expected the Fourier-transformed spectral and statistical functions exhibit the five peaks which can be approximated by Lorentzians, shown in Fig. 3 upper and middle panels. The inset shows the corresponding weights of the five Lorentzian peaks w-s. It is constructive to compare these spectra with the Fourier transform of the condensate particle imbalance (Fig. 3, lower panel). The red curve shows the Fourier transformed $z(t)$ in the strongly-coupled regime, i.e. for $t \lesssim \tau_f$. Surprisingly, it exhibits sizeable peaks roughly at energy positions of the five quasiparticle levels marked by vertical lines. This is a strong indication of the dynamically generated parametric resonance which governs this regime ($\tau_c \lesssim t \lesssim \tau_f$).

In the quasi-hydrodynamic regime ($t > \tau_f$) the behaviour is strikingly dissimilar. The condensate in this regime is expected to perform regular Josephson oscil-

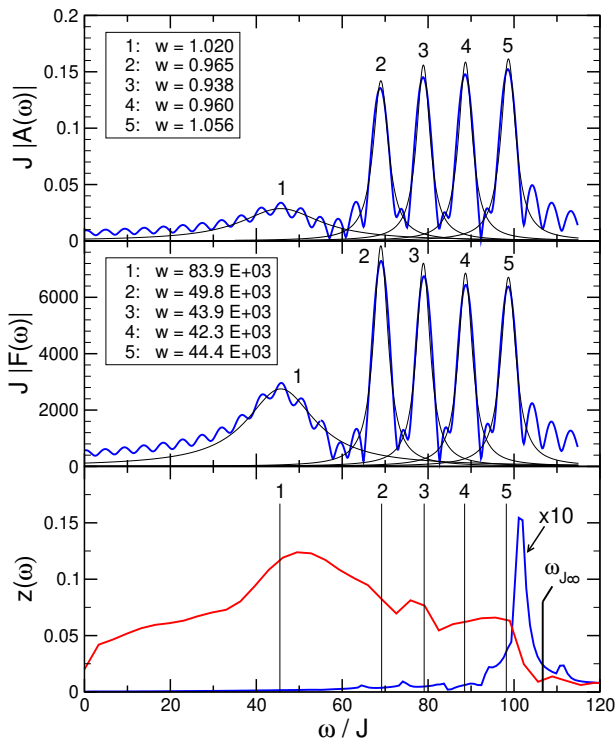


FIG. 3: Absolute values of spectral (upper panel) and statistical (middle panel) functions, Fourier transformed with respect to $(t-t')$ for a fixed value of $t_+ = (t+t')/2 = 9.01$ (in the units of $1/J$). The curves are fitted with Lorentzians, the weights w -s of the five Lorentzians are shown in the insets. In the lower panel the Fourier transformed particle imbalance $z(t)$ is shown for $\tau_c \lesssim t \lesssim \tau_f$ (red line) and for $t > \tau_f$ (blue line). The vertical lines indicate renormalized quasiparticle energies. $\omega_{J\infty}$ is the Josephson frequency estimated for the de

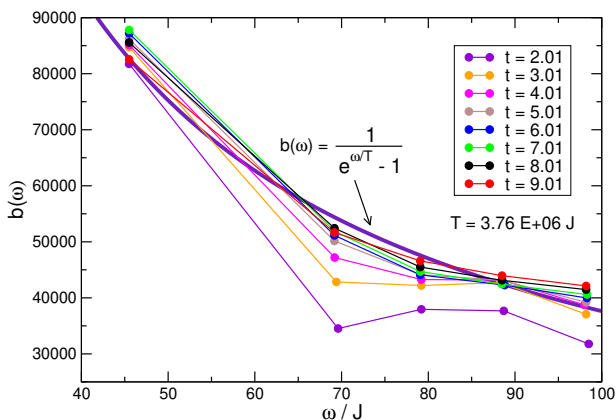


FIG. 4: Distribution function calculated from Eq. (11) for different center of mass time $t \equiv t_+$. The thick purple line is the two-parameter fit of the distribution curves for large t . T is the effective temperature of the final thermal state.

lations in accordance with semiclassical description [12],

which it indeed does. The difference, however, is that the Josephson coupling J is now strongly renormalized by the quasiparticle assisted tunnelling J' and is proportional to the total quasiparticle number n_{tot} . The renormalized Josephson frequency for the final state can be estimated as $\omega_{J\infty} \approx 2J_{eff} \sqrt{1 + uJ/(2J_{eff})}$, where $J_{eff} = J + n_{tot}J'$. We see that this frequency is indeed very close to the frequency of Josephson oscillations in the uncoupled regime (see the location of the blue peak in Fig. 3 lower panel), though not exactly equal to it because the condensates are not completely decoupled and the Josephson frequency is still influenced by the slower Rabi oscillations. Since the peak is no longer in resonance with the five quasiparticle peaks, we conclude the quasiparticle system is decoupled from the condensate in this regime. The sharpness of the condensate peak also indicates that the condensate oscillations are weakly damped.

Finally, we analyse thermalization of the distribution function

$$b(\omega, t_+) = \frac{|iF(\omega, t_+)|}{A(\omega, t_+)} - \frac{1}{2}. \quad (11)$$

for different values of the center of mass time t_+ (see Fig. 4). As expected, for small t_+ it does not show any signs of thermalisation. For large t_+ the distribution function however, approaches thermal distribution, whose temperature can be readily extracted.

To summarise, thermalisation in a finite isolated system is a nontrivial problem. Our system of coupled condensate and inflationary induced incoherent excitations thermalizes only because the condensate serves as a heat reservoir for the quasiparticles, at the same time being damped by the quasiparticle collisions. By studying system dynamics we found a coupling-decoupling crossover between the condensate and the quasiparticle systems at the time scale τ_f , which corresponds to the saturation of the total number of incoherent excitations determined by total energy conservation and as a result effective "freezing-out" of the condensate modes. Prior to τ_f condensate and quasiparticles are strongly coupled owing dynamically generated parametric resonance, which can be seen in the resonant spectra of BEC and quasiparticles. For $t > \tau_f$ BEC and incoherent excitations exhibit off-resonant behaviour and are effectively uncoupled. While off-resonant, the quasiparticle system slowly relaxes into a thermalized state (with thermalization time $\tau_{th} \gg \tau_f$). The BEC freeze-out and subsequent time evolution under a conservation law are reminiscent of "pre-thermalization" found in low-dimensional, integrable, or close to integrable systems. However, here the conservation law is generated dynamically in higher dimensional system. Curiously, the quasiparticle dynamics bears similarities to the inflationary creation of quantum fluctuations during the evolution of the early universe.

-
- [1] M. Rigol, V. Danjko, and M. Olshanii, *Nature* **452**, 854 (2007).
 - [2] A. Polkovnikov, K. Sengupta, A. Silva, and M. Vengalattore, *Rev. Mod. Phys.* **83**, 863 (2011).
 - [3] M. Gring, M. Kuhnert, T. Langen, T. Kitagawa, B. Rauer, M. Schreitl, I. Mazets, D. Adu Smith, E. Demler, and J. Schmiedmayer, *Science* **337**, 1318 (2012).
 - [4] M. Albiez *et al.*, *Phys. Rev. Lett.* **95**, 010402 (2005).
 - [5] S. Levy, E. Lahoud, I. Shomroni and J. Steinheuer, *Nature* **449**, 579 (2007).
 - [6] L. J. LeBlanc *et al.*, *Phys. Rev. Lett.* **106**, 025302 (2011).
 - [7] K. Sakmann, A. I. Streltsov, O. E. Alon, and L. S. Cederbaum, *Phys. Rev. Lett.* **103**, 220601 (2009).
 - [8] J. Rammer, *Quantum Field Theory of Non-equilibrium States*, Cambridge University Press 2007.
 - [9] A. Griffin, T. Nikuni, and E. Zaremba, *Bose-Condensed Gases at Finite Temperatures*, Cambridge University Press 2009.
 - [10] M. Trujillo-Martinez, A. Posazhennikova, and J. Kroha, *Phys. Rev. Lett.* **103**, 105302 (2009).
 - [11] M. Trujillo-Martinez, A. Posazhennikova, and J. Kroha, *New. J. Phys.* **17**, 013006 (2015).
 - [12] A. Smerzi, S. Fantoni, S. Giovanazzi, and S. R. Shenoy, *Phys. Rev. Lett.* **79**, 4950 (1997).

Supplementary Material for "Thermalisation of a quenched Bose Josephson junction due to inelastic collisions"

The supplementary material covers:

1. Quantum kinetic equations in the presence of inelastic collisions
2. Evaluation of the collisional second order self-energies and derivation of final equations
3. Notes on numerical calculations

I. KINETIC EQUATIONS IN THE PRESENCE OF INELASTIC COLLISIONS IN THE TRAP EIGENBASIS. FIRST ORDER SELF-ENERGIES

With the Hamiltonian (3) we can now derive kinetic equations of motion for the Green's functions of the condensate $\mathbf{C}(t, t')$ and quasi-particles $\mathbf{G}(t, t')$ in the trap eigenbasis. The Green's functions are defined as follows

$$\mathbf{C}_{\alpha\beta}(t, t') = -i \begin{pmatrix} a_{\alpha}(t)a_{\beta}^{*}(t') & a_{\alpha}(t)a_{\beta}(t') \\ a_{\alpha}^{*}(t)a_{\beta}^{*}(t') & a_{\alpha}^{*}(t)a_{\beta}(t') \end{pmatrix}, \quad (\text{S12})$$

$$\begin{aligned} \mathbf{G}_{nm}(t, t') &= -i \begin{pmatrix} \langle T_C \hat{b}_n(t) \hat{b}_m^{\dagger}(t') \rangle & \langle T_C \hat{b}_n(t) \hat{b}_m(t') \rangle \\ \langle T_C \hat{b}_n^{\dagger}(t) \hat{b}_m^{\dagger}(t') \rangle & \langle T_C \hat{b}_n^{\dagger}(t) \hat{b}_m(t') \rangle \end{pmatrix} \\ &= \begin{pmatrix} G_{nm}(t, t') & F_{nm}(t, t') \\ \bar{F}_{nm}(t, t') & \bar{G}_{nm}(t, t') \end{pmatrix}. \end{aligned} \quad (\text{S13})$$

The Dyson equations for these Green's functions have a standard form [11]. For the condensate Green's function it reads

$$\begin{aligned} \int_{-\infty}^{\infty} d\bar{t} [\mathbf{G}_{0,\alpha\gamma}^{-1}(t, \bar{t}) - \mathbf{S}_{\alpha\gamma}^{HF}(t, \bar{t})] \mathbf{C}_{\gamma\beta}(\bar{t}, t') = \quad (\text{S14}) \\ -i \int_{-\infty}^t d\bar{t} \gamma_{\alpha\gamma}(t, \bar{t}) \mathbf{C}_{\gamma\beta}(\bar{t}, t'). \end{aligned}$$

Here for convenience we write the self-energy as a sum of two terms: $\mathbf{S}_{\alpha\beta}^{cond} = \mathbf{S}_{\alpha\beta}^{HF} + \mathbf{S}_{\alpha\beta}$, where $\mathbf{S}_{\alpha\beta}^{HF}$ are the first order contributions (Bogoliubov-Hartree-Fock), whereas $\gamma_{\alpha\beta} = \mathbf{S}_{\alpha\beta}^{>} - \mathbf{S}_{\alpha\beta}^{<}$ are contributions responsible for collisions and therefore for equilibration of the system. All self-energies, including later appearing $\mathbf{\Gamma}$ and $\mathbf{\Pi}$ have the same 2×2 structure in the Bogoliubov space

$$\mathbf{S}(t, t') = \begin{pmatrix} S^G(t, t') & S^F(t, t') \\ S^{\bar{F}}(t, t') & S^{\bar{G}}(t, t') \end{pmatrix}. \quad (\text{S15})$$

The bare propagator is given by

$$\mathbf{G}_{0,\alpha\beta}^{-1}(t, t') = \left[i\tau_3 \delta_{\alpha\beta} \frac{\partial}{\partial t} - \mathbf{1} E_{\alpha\beta} \right] \delta(t - t'), \quad (\text{S16})$$

with $E_{11} = E_{22} = E_0$ and $E_{12} = E_{21} = -J$.

Instead of dealing with the quasi-particle Green's function \mathbf{G} , it is more convenient to work with spectral function \mathbf{A} and statistical function \mathbf{F} , which can be readily expressed via (S13) as $\mathbf{A}_{nm} = i(\mathbf{G}_{nm}^> - \mathbf{G}_{nm}^<)$ and $\mathbf{F}_{nm} = (\mathbf{G}_{nm}^> + \mathbf{G}_{nm}^<)/2 = \mathbf{G}_{nm}^K/2$ (with \mathbf{G}_{nm}^K being the Keldysh component of (S13), and $\mathbf{G}_{nm}^<$ and $\mathbf{G}_{nm}^>$ being the so-called lesser and greater components of the Green's function (S13) [8]):

$$\mathbf{A}_{nm}(t, t') = \begin{pmatrix} \mathbf{A}_{nm}^G(t, t') & \mathbf{A}_{nm}^F(t, t') \\ \mathbf{A}_{nm}^{\bar{F}}(t, t') & \mathbf{A}_{nm}^{\bar{G}}(t, t') \end{pmatrix}, \quad (\text{S17})$$

$$\mathbf{F}_{nm}(t, t') = \begin{pmatrix} \mathbf{F}_{nm}^G(t, t') & \mathbf{F}_{nm}^F(t, t') \\ \mathbf{F}_{nm}^{\bar{F}}(t, t') & \mathbf{F}_{nm}^{\bar{G}}(t, t') \end{pmatrix}. \quad (\text{S18})$$

Hereafter Greek indices, $\alpha, \beta = 1, 2$, refer to the condensates in the left and right wells, and latin indices, $n, m = 1, 2, \dots, M$, denote the QP levels, we also imply Einstein summation.

It is important to note that the functions (S22) and (S23) obey useful symmetry relations

$$\begin{aligned} \mathbf{A}^{\bar{G}}(t, t') &= -\mathbf{A}^G(t, t')^* = -\mathbf{A}^G(t', t), \\ \mathbf{A}^{\bar{F}}(t, t') &= -\mathbf{A}^F(t, t')^* = \mathbf{A}^F(t', t)^*, \\ \mathbf{F}^{\bar{G}}(t, t') &= -\mathbf{F}^G(t, t')^* = \mathbf{F}^G(t', t), \\ \mathbf{F}^{\bar{F}}(t, t') &= -\mathbf{F}^F(t, t')^* = -\mathbf{F}^F(t', t)^*. \end{aligned} \quad (\text{S19})$$

The Dyson equations for the spectral and statistical functions are

$$\int_{-\infty}^{\infty} d\bar{t} \left[\mathbf{G}_{0,n\ell}^{-1}(t, \bar{t}) - \Sigma_{n\ell}^{HF}(t, \bar{t}) \right] \mathbf{A}_{\ell m}(\bar{t}, t') = -i \int_{t'}^t d\bar{t} \mathbf{\Gamma}_{n\ell}(t, \bar{t}) \mathbf{A}_{\ell m}(\bar{t}, t') \quad (\text{S20})$$

$$\begin{aligned} \int_{-\infty}^{\infty} d\bar{t} \left[\mathbf{G}_{0,n\ell}^{-1}(t, \bar{t}) - \Sigma_{n\ell}^{HF}(t, \bar{t}) \right] \mathbf{F}_{\ell m}(\bar{t}, t') = \\ -i \left[\int_{-\infty}^t d\bar{t} \mathbf{\Gamma}_{n\ell}(t, \bar{t}) \mathbf{F}_{\ell m}(\bar{t}, t') \right. \\ \left. - \int_{-\infty}^{t'} d\bar{t} \mathbf{\Pi}_{n\ell}(t, \bar{t}) \mathbf{A}_{\ell m}(\bar{t}, t') \right], \end{aligned} \quad (\text{S21})$$

where $\mathbf{\Pi}_{nm} = (\Sigma_{nm}^> + \Sigma_{nm}^<)/2$ and $\mathbf{\Gamma}_{nm} = \Sigma_{nm}^> - \Sigma_{nm}^<$ and are 2×2 matrices in the Bogoliubov space

$$\mathbf{\Gamma}_{nm}(t, t') = \begin{pmatrix} \mathbf{\Gamma}_{nm}^G(t, t') & \mathbf{\Gamma}_{nm}^F(t, t') \\ \mathbf{\Gamma}_{nm}^{\bar{F}}(t, t') & \mathbf{\Gamma}_{nm}^{\bar{G}}(t, t') \end{pmatrix}, \quad (\text{S22})$$

$$\mathbf{\Pi}_{nm}(t, t') = \begin{pmatrix} \mathbf{\Pi}_{nm}^G(t, t') & \mathbf{\Pi}_{nm}^F(t, t') \\ \mathbf{\Pi}_{nm}^{\bar{F}}(t, t') & \mathbf{\Pi}_{nm}^{\bar{G}}(t, t') \end{pmatrix}. \quad (\text{S23})$$

Here again we separate out the Bogoliubov-Hartree-Fock contributions Σ_{nm}^{HF} from the second-order contributions describing collisions Σ_{nm} .

The bare one-particle propagator and the Hartree-Fock self-energy is given by

$$\mathbf{G}_{0,nm}^{-1}(t, t') = \left[i\tau_3 \frac{\partial}{\partial t} - \epsilon_n \mathbf{1} \right] \delta_{nm} \delta(t - t'), \quad (\text{S24})$$

The Hartree-Fock self-energies are 2×2 matrices in Bogoliubov space and depend only on one time argument $\mathbf{S}^{HF}(t, t') = \mathbf{S}^{HF}(t) \delta(t - t')$, $\Sigma^{HF}(t, t') = \Sigma^{HF}(t) \delta(t - t')$

$$\mathbf{S}_{\alpha\beta}^{HF}(t) = \begin{pmatrix} S_{\alpha\beta}^{HF}(t) & W_{\alpha\beta}^{HF}(t) \\ W_{\alpha\beta}^{HF}(t)^* & S_{\alpha\beta}^{HF}(t)^* \end{pmatrix}, \quad (\text{S25})$$

$$\Sigma_{nm}^{HF}(t) = \begin{pmatrix} \Sigma_{nm}^{HF}(t) & \Omega_{nm}^{HF}(t) \\ \Omega_{nm}^{HF}(t)^* & \Sigma_{nm}^{HF}(t)^* \end{pmatrix}. \quad (\text{S26})$$

\mathbf{S}^{HF} and Σ^{HF} contain contributions proportional to U, J' and K and describe the dynamical shift of the condensate and the single-particle levels due to the dynamical change of their occupation numbers and their interactions:

$$\begin{aligned} \mathbf{S}_{\alpha\alpha}^{HF}(t) &= \frac{i}{2} U \text{Tr} [\mathbf{C}_{\alpha\alpha}(t, t)] \mathbf{1} + \\ & i \frac{K}{2} \sum_{n,m=1}^M \left\{ \frac{1}{2} \text{Tr} [\mathbf{F}_{nm}^<(t, t)] \mathbf{1} + \mathbf{F}_{nm}^<(t, t) \right\} \\ \mathbf{S}_{12}^{HF}(t, t') &= \mathbf{S}_{21}^{HF}(t, t') = \\ & i \frac{J'}{2} \sum_{n,m=1}^M \left\{ \frac{1}{2} \text{Tr} [\mathbf{F}_{nm}^<(t, t)] \mathbf{1} + \mathbf{F}_{nm}^<(t, t) \right\}, \end{aligned} \quad (\text{S27})$$

and

$$\begin{aligned} \Sigma_{nm}^{HF}(t, t') &= i \frac{K}{2} \sum_{\alpha} \left\{ \mathbf{C}_{\alpha\alpha}(t, t) + \frac{1}{2} \text{Tr} [\mathbf{C}_{\alpha\alpha}(t, t)] \mathbf{1} \right\} \\ &+ i \frac{J'}{2} \sum_{\alpha \neq \beta} \left\{ \mathbf{C}_{\alpha\beta}(t, t) + \frac{1}{2} \text{Tr} [\mathbf{C}_{\alpha\beta}(t, t)] \mathbf{1} \right\} \\ &+ i U' \sum_{\ell,s=1}^M \left\{ \mathbf{F}_{\ell s}(t, t) + \frac{1}{2} \text{Tr} [\mathbf{F}_{\ell s}(t, t)] \mathbf{1} \right\} \end{aligned} \quad (\text{S28})$$

where ϵ_n are equidistant eigenenergies of the trap, $\epsilon_2 = \epsilon_1 + \Delta$ and so on.

Evaluation of the integrals on the left-hand side of the Dyson equations gives

$$\begin{aligned} \left[i\tau_3 \delta_{\alpha\gamma} \frac{\partial}{\partial t} - \mathbf{1} E_{\alpha\gamma} - \mathbf{S}_{\alpha\gamma}^{HF}(t) \right] \mathbf{C}_{\gamma\beta}(t, t') = \\ -i \int_{-\infty}^t d\bar{t} \gamma_{\alpha\gamma}(t, \bar{t}) \mathbf{C}_{\gamma\beta}(\bar{t}, t'), \end{aligned} \quad (\text{S29})$$

$$\left[i\tau_3 \delta_{nl} \frac{\partial}{\partial t} - \epsilon_n \delta_{nl} \mathbb{1} - \Sigma_{nl}^{HF}(t) \right] \mathbf{A}_{\ell m}(t, t') = -i \int_{t'}^t d\bar{t} \Gamma_{nl}(t, \bar{t}) \mathbf{A}_{\ell m}(\bar{t}, t'), \quad (\text{S30})$$

$$\left[i\tau_3 \delta_{nl} \frac{\partial}{\partial t} - \epsilon_n \delta_{nl} \mathbb{1} - \Sigma_{nl}^{HF}(t) \right] \mathbf{F}_{\ell m}(t, t') = -i \left[\int_{-\infty}^t d\bar{t} \Gamma_{nl}(t, \bar{t}) \mathbf{F}_{\ell m}(\bar{t}, t') - \int_{-\infty}^{t'} d\bar{t} \Pi_{nl}(t, \bar{t}) \mathbf{A}_{\ell m}(\bar{t}, t') \right]. \quad (\text{S31})$$

Eqs. (S29), (S30) and (S31) constitute the general equations of motion for the condensate and the non-condensate (spectral and statistical) propagators. They are coupled via the self-energies which are functions of these propagators and must be evaluated self-consistently in order to obtain a conserving approximation. The higher order interaction terms on the right-hand side of the equations of motion describe inelastic quasi-particle collisions. They are, in general, responsible for quasi-particle damping, damping of the condensate oscillations and for thermalization. We consider them in detail in the next section.

II. EVALUATION OF THE SECOND ORDER CONTRIBUTIONS TO SELF-ENERGIES DUE TO COLLISIONS

The collisional terms are taken into account within the full second order approximation. Due to the symmetry relation (S19) we can express the collisional self-energies in terms of only upper left and upper right components of the spectral function $\mathbf{A}_{nm}(t, t')$ and the statistical function $\mathbf{F}_{nm}(t, t')$. We obtain for γ in (S29)

$$\begin{aligned} \gamma_{\alpha\alpha'}^G(t, t') &= R^2 \sum_{nls} \sum_{n'l's'} \left(\mathbf{F}_{nn'}^G(t, t') \left\{ 4\Lambda_{ss'}^{\ell\ell'}[\mathbf{F}, \mathbf{F}^*](t, t') \right. \right. \\ &\quad \left. \left. + 2\Lambda_{ss'}^{\ell\ell'}[\mathbf{G}, \mathbf{G}^*](t, t') \right\} \right. \\ &\quad \left. + \mathbf{A}_{nn'}^G(t, t') \left\{ 4\Xi_{ss'}^{\ell\ell'}[\mathbf{F}, \mathbf{F}^*](t, t') + 2\Xi_{ss'}^{\ell\ell'}[\mathbf{G}, \mathbf{G}^*](t, t') \right\} \right) \\ \gamma_{\alpha\alpha'}^F(t, t') &= R^2 \sum_{nls} \sum_{n'l's'} \left(\mathbf{F}_{nn'}^F(t, t') \left\{ 4\Lambda_{ss'}^{\ell\ell'}[\mathbf{G}, \mathbf{G}^*](t, t') \right. \right. \\ &\quad \left. \left. + 2\Lambda_{ss'}^{\ell\ell'}[\mathbf{F}, \mathbf{F}^*](t, t') \right\} \right. \\ &\quad \left. + \mathbf{A}_{nn'}^F(t, t') \left\{ 4\Xi_{ss'}^{\ell\ell'}[\mathbf{G}, \mathbf{G}^*](t, t') + 2\Xi_{ss'}^{\ell\ell'}[\mathbf{F}, \mathbf{F}^*](t, t') \right\} \right). \end{aligned} \quad (\text{S32})$$

Here we introduced for the sake of shorter notations

$$\begin{aligned} \Lambda_{ss'}^{\ell\ell'}[\mathbf{G}, \mathbf{F}](t, t') &= \mathbf{A}_{\ell\ell'}^G(t, t') \mathbf{F}_{ss'}^F(t, t') + \mathbf{F}_{\ell\ell'}^G(t, t') \mathbf{A}_{ss'}^F(t, t') \\ \Lambda_{ss'}^{\ell\ell'}[\mathbf{G}, \mathbf{G}^*](t, t') &= \mathbf{A}_{\ell\ell'}^G(t, t') \mathbf{F}_{ss'}^G(t, t')^* + \mathbf{F}_{\ell\ell'}^G(t, t') \mathbf{A}_{ss'}^G(t, t')^* \\ \Xi_{ss'}^{\ell\ell'}[\mathbf{G}, \mathbf{F}](t, t') &= \mathbf{F}_{ss'}^G(t, t') \mathbf{F}_{ss'}^F(t, t') - \frac{1}{4} \mathbf{A}_{\ell\ell'}^G(t, t') \mathbf{A}_{ss'}^F(t, t') \\ \Xi_{ss'}^{\ell\ell'}[\mathbf{G}, \mathbf{G}^*](t, t') &= \mathbf{F}_{\ell\ell'}^G(t, t') \mathbf{F}_{ss'}^G(t, t')^* - \frac{1}{4} \mathbf{A}_{\ell\ell'}^G(t, t') \mathbf{A}_{ss'}^G(t, t')^* \end{aligned}$$

and so on. The remaining γ -s are related to γ^G and γ^F by symmetry relations

$$\begin{aligned} \gamma^G(t, t')^* &= -\gamma^{\bar{G}}(t, t') = \gamma^G(t', t), \\ \gamma^F(t, t')^* &= -\gamma^{\bar{F}}(t, t') = \gamma^F(t', t). \end{aligned} \quad (\text{S33})$$

For Γ we get

$$\begin{aligned} \Gamma_{nn'}^G(t, t') &= 2iR^2 \sum_{\alpha\ell s} \sum_{\alpha'\ell's'} \left(2a_\alpha^*(t) a_{\alpha'}(t') \Lambda_{ss'}^{\ell\ell'}[\mathbf{G}, \mathbf{F}](t, t') \right. \\ &\quad \left. + a_\alpha^*(t) a_{\alpha'}(t') \Lambda_{ss'}^{\ell\ell'}[\mathbf{G}, \mathbf{G}](t, t') \right. \\ &\quad \left. - 2a_\alpha(t) a_{\alpha'}(t') \Lambda_{ss'}^{\ell\ell'}[\mathbf{F}^*, \mathbf{G}](t, t') \right. \\ &\quad \left. - 2a_\alpha(t) a_{\alpha'}(t') \left\{ \Lambda_{ss'}^{\ell\ell'}[\mathbf{G}, \mathbf{G}^*](t, t') + \Lambda_{ss'}^{\ell\ell'}[\mathbf{F}, \mathbf{F}^*](t, t') \right\} \right) \\ &\quad + (U')^2 \sum_{m\ell s} \sum_{m'\ell's'} \left(\mathbf{F}_{mm'}^G(t, t') \left\{ 4\Lambda_{ss'}^{\ell\ell'}[\mathbf{F}, \mathbf{F}^*](t, t') \right. \right. \\ &\quad \left. \left. + 2\Lambda_{ss'}^{\ell\ell'}[\mathbf{G}, \mathbf{G}^*](t, t') \right\} \right. \\ &\quad \left. + \mathbf{A}_{mm'}^G(t, t') \left\{ 4\Xi_{ss'}^{\ell\ell'}[\mathbf{F}, \mathbf{F}^*](t, t') + 2\Xi_{ss'}^{\ell\ell'}[\mathbf{G}, \mathbf{G}^*](t, t') \right\} \right) \end{aligned} \quad (\text{S34})$$

and

$$\begin{aligned} \Gamma_{nn'}^F(t, t') &= 2iR^2 \sum_{\alpha\ell s} \sum_{\alpha'\ell's'} \left(2a_\alpha^*(t) a_{\alpha'}(t') \Lambda_{ss'}^{\ell\ell'}[\mathbf{G}, \mathbf{F}](t, t') \right. \\ &\quad \left. + a_\alpha^*(t) a_{\alpha'}(t') \Lambda_{ss'}^{\ell\ell'}[\mathbf{F}, \mathbf{F}](t, t') \right. \\ &\quad \left. - 2a_\alpha(t) a_{\alpha'}(t') \Lambda_{ss'}^{\ell\ell'}[\mathbf{G}^*, \mathbf{F}](t, t') \right. \\ &\quad \left. - 2a_\alpha(t) a_{\alpha'}(t') \left\{ \Lambda_{ss'}^{\ell\ell'}[\mathbf{G}, \mathbf{G}^*](t, t') + \Lambda_{ss'}^{\ell\ell'}[\mathbf{F}, \mathbf{F}^*](t, t') \right\} \right) \\ &\quad + (U')^2 \sum_{m\ell s} \sum_{m'\ell's'} \left(\mathbf{F}_{mm'}^F(t, t') \left\{ 2\Lambda_{ss'}^{\ell\ell'}[\mathbf{F}, \mathbf{F}^*](t, t') \right. \right. \\ &\quad \left. \left. + 4\Lambda_{ss'}^{\ell\ell'}[\mathbf{G}, \mathbf{G}^*](t, t') \right\} \right. \\ &\quad \left. + \mathbf{A}_{mm'}^F(t, t') \left\{ 2\Xi_{ss'}^{\ell\ell'}[\mathbf{F}, \mathbf{F}^*](t, t') + 4\Xi_{ss'}^{\ell\ell'}[\mathbf{G}, \mathbf{G}^*](t, t') \right\} \right). \end{aligned} \quad (\text{S35})$$

Other self-energy parts in the Dyson equation for the

statistical function have the following contributions

$$\begin{aligned}
\Pi_{nn'}^G(t, t') &= 2iR^2 \sum_{\alpha l s} \sum_{\alpha' l' s'} \left(2a_{\alpha}^*(t) a_{\alpha'}^*(t') \Xi_{ss'}^{\ell \ell'} [G, F](t, t') \right. \\
&+ a_{\alpha}^*(t) a_{\alpha'}^*(t') \Xi_{ss'}^{\ell \ell'} [G, G](t, t') \\
&- 2a_{\alpha}(t) a_{\alpha'}(t') \Xi_{ss'}^{\ell \ell'} [F^*, G](t, t') \\
&- 2a_{\alpha}(t) a_{\alpha'}^*(t') \left\{ \Xi_{ss'}^{\ell \ell'} [G, G^*](t, t') + \Xi_{ss'}^{\ell \ell'} [F, F^*](t, t') \right\} \\
&+ (U')^2 \sum_{m l s} \sum_{m' l' s'} \left(F_{mm'}^G(t, t') \left\{ 4\Xi_{ss'}^{\ell \ell'} [F, F^*](t, t') \right. \right. \\
&+ 2\Xi_{ss'}^{\ell \ell'} [G, G^*](t, t') \left. \left. \right\} \right. \\
&- \left. \frac{1}{2} A_{mm'}^G(t, t') \left\{ 2\Lambda_{ss'}^{\ell \ell'} [F, F^*](t, t') + \Lambda_{ss'}^{\ell \ell'} [G, G^*](t, t') \right\} \right) \quad (S36)
\end{aligned}$$

and

$$\begin{aligned}
\Pi_{nn'}^F(t, t') &= 2iR^2 \sum_{\alpha l s} \sum_{\alpha' l' s'} \left(2a_{\alpha}^*(t) a_{\alpha'}^*(t') \Xi_{ss'}^{\ell \ell'} [G, F](t, t') \right. \\
&+ a_{\alpha}^*(t) a_{\alpha'}^*(t') \Xi_{ss'}^{\ell \ell'} [F, F](t, t') \\
&- 2a_{\alpha}(t) a_{\alpha'}^*(t') \Xi_{ss'}^{\ell \ell'} [G^*, F](t, t') \\
&- 2a_{\alpha}(t) a_{\alpha'}(t') \left\{ \Xi_{ss'}^{\ell \ell'} [G, G^*](t, t') + \Xi_{ss'}^{\ell \ell'} [F, F^*](t, t') \right\} \\
&+ (U')^2 \sum_{m l s} \sum_{m' l' s'} \left(F_{mm'}^F(t, t') \left\{ 2\Xi_{ss'}^{\ell \ell'} [F, F^*](t, t') \right. \right. \\
&+ 4\Xi_{ss'}^{\ell \ell'} [G, G^*](t, t') \left. \left. \right\} \right. \\
&- \left. \frac{1}{2} A_{mm'}^F(t, t') \left\{ \Lambda_{ss'}^{\ell \ell'} [F, F^*](t, t') + 2\Lambda_{ss'}^{\ell \ell'} [G, G^*](t, t') \right\} \right). \quad (S37)
\end{aligned}$$

The following symmetry relations apply here

$$\begin{aligned}
\Gamma^G(t, t')^* &= -\Gamma^{\bar{G}}(t, t') = \Gamma^G(t', t), \\
\Gamma^F(t, t')^* &= -\Gamma^{\bar{F}}(t, t') = \Gamma^F(t', t), \\
\Pi^G(t, t')^* &= -\Pi^{\bar{G}}(t, t') = -\Pi^G(t', t), \\
\Pi^F(t, t')^* &= -\Pi^{\bar{F}}(t, t') = -\Pi^F(t', t). \quad (S38)
\end{aligned}$$

Because of the symmetry relations (S19) we can express all quantities appearing in the equations of motion with the later time argument on the left side. Final equations of motion for the spectral function are

$$\begin{aligned}
i \frac{\partial}{\partial t} A_{nm}^G(t, t') &= (\epsilon_n \delta_{nl} + \Sigma_{nl}^{HF}) A_{\ell m}^G(t, t') \\
&- \Omega_{nl}^{HF}(t) (A_{\ell m}^F(t, t'))^* \\
-i \int_{t'}^t d\bar{t} &\left[\Gamma_{n\ell}^G(t, \bar{t}) A_{\ell m}^G(\bar{t}, t') + \Gamma_{n\ell}^F(t, \bar{t}) A_{\ell m}^{\bar{F}}(\bar{t}, t') \right] \\
i \frac{\partial}{\partial t} A_{nm}^F(t, t') &= (\epsilon_n \delta_{nl} + \Sigma_{nl}^{HF}) A_{\ell m}^F(t, t') \\
&- \Omega_{nl}^{HF}(t) (A_{\ell m}^G(t, t'))^* \\
-i \int_{t'}^t d\bar{t} &\left[\Gamma_{n\ell}^G(t, \bar{t}) A_{\ell m}^F(\bar{t}, t') + \Gamma_{n\ell}^F(t, \bar{t}) A_{\ell m}^{\bar{G}}(\bar{t}, t') \right] \quad (S39)
\end{aligned}$$

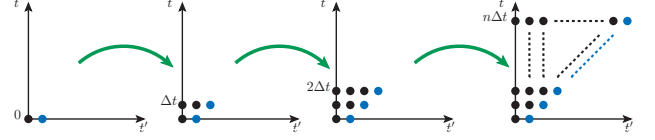


FIG. S5: Time plane grid.

For the statistical function we get

$$\begin{aligned}
i \frac{\partial}{\partial t} F_{nm}^G(t, t') &= (\epsilon_n \delta_{nl} + \Sigma_{nl}^{HF}) F_{\ell m}^G(t, t') \\
&- \Omega_{nl}^{HF}(t) (F_{\ell m}^F(t, t'))^* \\
-i \int_0^t d\bar{t} &\left[\Gamma_{n\ell}^G(t, \bar{t}) F_{\ell m}^G(\bar{t}, t') + \Gamma_{n\ell}^F(t, \bar{t}) F_{\ell m}^{\bar{F}}(\bar{t}, t') \right] \\
+i \int_0^t d\bar{t} &\left[\Pi_{n\ell}^G(t, \bar{t}) A_{\ell m}^G(\bar{t}, t') + \Pi_{n\ell}^F(t, \bar{t}) A_{\ell m}^{\bar{F}}(\bar{t}, t') \right] \\
i \frac{\partial}{\partial t} F_{nm}^F(t, t') &= (\epsilon_n \delta_{nl} + \Sigma_{nl}^{HF}) F_{\ell m}^F(t, t') \\
&- \Omega_{nl}^{HF}(t) (F_{\ell m}^G(t, t'))^* \\
-i \int_0^t d\bar{t} &\left[\Gamma_{n\ell}^G(t, \bar{t}) F_{\ell m}^F(\bar{t}, t') + \Gamma_{n\ell}^F(t, \bar{t}) F_{\ell m}^{\bar{G}}(\bar{t}, t') \right] \\
+i \int_0^t d\bar{t} &\left[\Pi_{n\ell}^G(t, \bar{t}) A_{\ell m}^F(\bar{t}, t') + \Pi_{n\ell}^F(t, \bar{t}) A_{\ell m}^{\bar{G}}(\bar{t}, t') \right] \quad (S40)
\end{aligned}$$

The equations (S39) and (S40) are coupled to the equations of motion for the condensates amplitudes

$$\begin{aligned}
i \frac{\partial}{\partial t} a_{\alpha}(t) &= -J a_{\beta \neq \alpha}(t) + S_{\alpha\beta}^{HF} a_{\beta}(t) + W_{\alpha\beta}^{HF} a_{\beta}^*(t) \\
-i \int_0^t d\bar{t} &\left[\gamma_{\alpha\beta}^G(t, \bar{t}) a_{\beta}(\bar{t}) + \gamma_{\alpha\beta}^F(t, \bar{t}) a_{\beta}^*(\bar{t}) \right]. \quad (S41)
\end{aligned}$$

Equations (S39), (S40) and (S41) are then solved numerically for various values of U, U', J and R .

III. NOTES ON NUMERICAL CALCULATIONS

In order to solve numerically our system of integro-differential equations, we discretize the two time arguments, t and t' with a constant time-step Δt (see Fig. S5). As a result, our spectral and statistical functions become matrices in the two-dimensional time plane. For instance,

$$F(t, t') = \begin{pmatrix} F(0, 0) & F(0, \Delta t) & \cdots & F(0, n\Delta t) \\ F(\Delta t, 0) & F(\Delta t, \Delta t) & \cdots & F(\Delta t, n\Delta t) \\ \vdots & \vdots & \ddots & \vdots \\ F(n\Delta t, 0) & F(n\Delta t, \Delta t) & \cdots & F(n\Delta t, n\Delta t) \end{pmatrix} \quad (S42)$$

where both time arguments are counted from τ_c , which is a finite time-scale at which the nonequilibrium dynamics

sets in [11], so that $F^G(0,0) \equiv F^G(\tau_c, \tau_c)$ etc. Both time scales go up to $t_{max} = n\Delta t$. In our case $t_{max} = 10$. Fortunately, due to the symmetry relations (S19) it is sufficient to calculate only half of the components of our propagators, i.e. the triangular matrix

$$F(t, t')_{tri} = \begin{pmatrix} F(0,0) & F(0,\Delta t) & \cdots & F(0,n\Delta t) \\ 0 & F(\Delta t, \Delta t) & \cdots & F(\Delta t, n\Delta t) \\ \vdots & \vdots & \ddots & \vdots \\ 0 & 0 & \cdots & F(n\Delta t, n\Delta t), \end{pmatrix} \quad (\text{S43})$$

which is reflected in the time-plane grid in Fig.S5. The blue points on the grid constitute additional copies of the diagonal (propagators with equal time arguments) contributions, necessary to properly perform the fourth order Runge-Kutta method. Symmetry relations for the self-energies (S38) also contribute to simplifications, as we can rewrite all the integrands in Eqs. (S39), (S40) with time argument corresponding to later time on the left, e.g. time convolutions in the equation of motion for F^G can be rewritten as

$$\begin{aligned} & -i \int_0^t d\bar{t} \left[\Gamma_{n\ell}^G(t, \bar{t}) F_{\ell m}^G(\bar{t}, t') + \Gamma_{n\ell}^F(t, \bar{t}) F_{\ell m}^{\bar{F}}(\bar{t}, t') \right] \\ & +i \int_0^t d\bar{t} \left[\Pi_{n\ell}^G(t, \bar{t}) A_{\ell m}^G(\bar{t}, t') + \Pi_{n\ell}^F(t, \bar{t}) A_{\ell m}^{\bar{F}}(\bar{t}, t') \right] \\ = & i \int_0^{t'} d\bar{t} \left[\Gamma_{n\ell}^G(t, \bar{t}) F_{\ell m}^G(t', \bar{t})^* + \Gamma_{n\ell}^F(t, \bar{t}) F_{\ell m}^F(t', \bar{t})^* \right] \\ & -i \int_{t'}^t d\bar{t} \left[\Gamma_{n\ell}^G(t, \bar{t}) F_{\ell m}^G(\bar{t}, t') - \Gamma_{n\ell}^F(t, \bar{t}) F_{\ell m}^F(\bar{t}, t')^* \right] \\ & +i \int_0^{t'} d\bar{t} \left[\Pi_{n\ell}^G(t, \bar{t}) A_{\ell m}^G(t', \bar{t})^* + \Pi_{n\ell}^F(t, \bar{t}) A_{\ell m}^F(t', \bar{t})^* \right] \end{aligned} \quad (\text{S44})$$

In nonequilibrium it is conventional to introduce mixed or Wigner coordinates: $\tau = t - t'$ and $T = (t + t')/2$ and then Fourier transform spectral functions and statistical functions with respect to the relative coordinate. In this way one can extract information about spectrum and distribution function for different values of T and check if system approaches equilibrium with increasing T . In our case it is done by reading off the calculated spectral and statistical functions belonging to diagonals with the slope equal to -1 from the $t - t'$ plane in Fig. S5. Those will be data for fixed T -s. We then Fourier transform them with respect to τ .